A new approach for studying the hydrodynamic stability of fluids with microstructure

Madan Somasi and Bamin Khomami[a)]
Department of Chemical Engineering and The Materials Research Laboratory, Washington University, St. Louis, Missouri 63130-4899

(Received 9 May 2000; accepted 30 January 2001)

A new methodology for studying the stability of fluids with microstructure has been developed. This technique relies on combining continuum based conservation equations and stochastic simulation techniques to determine the hydrodynamic stability of flows under consideration. To illustrate the capability of the method, the stability of viscoelastic Taylor–Couette flow has been examined. © *2001 American Institute of Physics.* [DOI: 10.1063/1.1369126]

Understanding the stability and dynamics of fluids with microstructure such as viscoelastic fluids has proved to be a great challenge for researchers over the last couple of decades.[1,2] Traditionally, the linear stability analyses of these flows have been carried out by solving the generalized eigenvalue problem (GEVP) resulting from normal-mode analysis or time-dependent simulations. However, both these techniques suffer from an inherent need for a closed-form constitutive equation (CCE) to describe the relationship between fluid stresses and the deformation rate. While most of these CCEs for fluids with microstructure originate from models based on statistical mechanics, the final CCE itself is derived by invoking various ''closure'' approximations. However, these approximations can sometimes distort the actual model behavior to a significant extent. For example, the stress conformation hysteresis seen in uniaxial extensional flows of polymeric solutions can be captured by Brownian dynamics of finitely extensible spring models, but the corresponding macroscopic equation derived by making closure approximations does not display this hysteretic behavior seen in experiments.[3]

Recently, a new methodology for performing flow simulations of fluids with a microstructure has emerged. For example, simulations of viscoelastic flows are performed by combining solution of macroscopic equations such as conservation of mass and momentum with kinetic theory based models for determination of the polymeric stresses.[4] In this study, we have developed a new technique that uses a combined finite element/Brownian dynamics approach to examine the hydrodynamic stability of fluids with microstructure. The principal motivation behind this work has been to develop a technique that will allow one to determine the hydrodynamic stability of fluids with microstructure without invoking closure approximations. In particular, we shall be looking at the stability of Taylor–Couette flow of polymer solutions modeled as a noninteracting suspension of elastic dumbbells. The Taylor–Couette geometry has been chosen because it is one of the most widely studied stability problems in the viscoelastic flow community[1,2,5] and is hence a very good paradigm to demonstrate our technique.

Taylor–Couette flow is essentially the flow in the annular region of two infinitely long, coaxial cylinders of radii R_1 and R_2 either or both of which can be rotating with angular speeds Ω_1 and Ω_2, respectively. In the present work, we shall be concerned with the case in which only the inner cylinder is rotating, i.e., $\Omega_2 \equiv 0$. It is well known that this flow becomes unstable once a critical value of the Deborah number, characterizing the relative importance of the elasticity and flow time scales of the fluid, is exceeded. This instability manifests itself as toroidal vortices in the axial directions in an otherwise azimuthal base flow. The governing equations for creeping flow of an incompressible fluid in the absence of body forces are

$$-\nabla P + \nabla \cdot \boldsymbol{\tau} = 0, \tag{1}$$

$$\nabla \cdot \boldsymbol{u} = 0, \tag{2}$$

where P, $\boldsymbol{\tau}$, and $\boldsymbol{u}$ are the fluid pressure, deviatoric stress tensor, and the velocity vector, respectively. The characteristic scales are the gap width $d = R_2 - R_1$, the velocity at the inner cylinder $\Omega_1 R_1$ and $d/\Omega_1 R_1$ for length, velocity, and time, respectively. The radii ratio is set to $\delta \equiv R_1/R_2 = 0.912$ in order to facilitate comparisons with previous studies.[5] The stress and the pressure variables have been made dimensionless by $\eta_0 \Omega_1 R_1/d$ where $\eta_0 = \eta_s + \eta_p$ is the total solution viscosity with η_s and η_p being the solvent and the polymer viscosity, respectively. As is common in viscoelastic flow simulations, the stress is split into a polymer and solvent contribution, i.e., $\boldsymbol{\tau} = \boldsymbol{\tau}_s + \boldsymbol{\tau}_p$. The solvent contribution is assumed to be Newtonian, $\boldsymbol{\tau}_s = 2\beta\dot{\gamma}$, where $\dot{\gamma} = \frac{1}{2}(\nabla \boldsymbol{u} + \nabla \boldsymbol{u}^{\dagger})$ is the rate of deformation tensor and $\beta = \eta_s/\eta_0$ denotes the solvent viscosity ratio. The system of equations [Eq. (1) and (2)] is closed by either selecting a closed form constitutive equation for the polymeric stress or by evaluating the polymeric stress as an appropriate expectation from an ensemble of model polymers. The closed form constitutive equation used in this study is the Oldroyd-B model in which the polymeric contribution to the stress, $\boldsymbol{\tau}_p$, is given as

a)Author to whom correspondence should be addressed. Telephone: (314) 935-6065; Fax: (314) 935-7211. Electronic mail: bam@poly1.che.wustl.edu

$$\boldsymbol{\tau}_p + \mathrm{De}\boldsymbol{\tau}_{p(1)} = 2(1-\beta)\dot{\gamma},$$

where $\mathrm{De} = \lambda\Omega_1 R_1/d$ is the Deborah number with λ being the relaxation time of the polymer. The subscript (1) denotes the upper-convected derivative, which is defined as

$$\boldsymbol{\tau}_{p(1)} = \frac{\partial \boldsymbol{\tau}_p}{\partial t} + \boldsymbol{u}\cdot\nabla\boldsymbol{\tau}_p - \boldsymbol{\kappa}\cdot\boldsymbol{\tau}_p - \boldsymbol{\tau}_p\cdot\boldsymbol{\kappa}^{\dagger},$$

where $\boldsymbol{\kappa}$ is the transpose of the velocity gradient (i.e., $\boldsymbol{\kappa} = \nabla\boldsymbol{u}^{\dagger}$). The kinetic theory based models used are the Hookean and the FENE (Finitely Extensible Non-linear Elastic) dumbbell models.[6] Both the models consist of elastic dumbbells having two Brownian beads attached by an entropic spring. For the Hookean dumbbell, a linear spring connects the two beads such that $\boldsymbol{F}^c = \boldsymbol{Q}$ whereas for the FENE dumbbell, we have a non-linear spring force law of the form $\boldsymbol{F}^c = \boldsymbol{Q}/(1-Q^2/b)$. In the above expressions, $\boldsymbol{Q}$ is the vector connecting the two beads, Q is the length of the connector and b is the maximum extensibility of the spring. Note that $b\to\infty$ for Hookean dumbbells because of their infinite extensibility. Another difference between the two models is the fact that only the Hookean dumbbell renders itself to an exact CCE, namely the Oldroyd-B model. In both the models, the evolution of the connector vector is modeled using the method of Brownian configurational fields,[7] according to the following stochastic differential equation (SDE):

$$d\boldsymbol{Q} = \left[-\boldsymbol{u}\cdot\boldsymbol{Q} + \boldsymbol{\kappa}\cdot\boldsymbol{Q} - \frac{1}{2\mathrm{De}}\boldsymbol{F}^c\right]dt + \sqrt{\frac{1}{\mathrm{De}}}\,d\boldsymbol{W}(t),$$

where $d\boldsymbol{W}(t)$ is a Wiener process which accounts for the Brownian force experienced by the beads. The Wiener process is a Gaussian random vector with zero mean and variance Δt, the discretization for the time interval.

Once all the $\boldsymbol{Q}$s have been evaluated, the polymeric stress can be obtained by invoking the Kramer's expression

$$\boldsymbol{\tau}_p = \frac{(1-\beta)}{\mathrm{De}}\left(\frac{b+5}{b}\right)(\langle\boldsymbol{F}^c\boldsymbol{Q}\rangle - \langle\boldsymbol{F}^c\boldsymbol{Q}\rangle_{eqbm}),$$

where $\langle\boldsymbol{F}^c\boldsymbol{Q}\rangle_{eqbm} = \boldsymbol{\delta}$, the unit tensor. We have used a specialized finite element method, namely the DEVSS-G/SUPG (Discrete Elastic Viscous Split Stress—Gradient of Velocity/Streamline Upwind Petrov–Galerkin) that has been shown to provide an accurate discretization for viscoelastic flows with a predictor-corrector type of discretization in time to solve the set of governing equations. The exact details of the scheme and its advantages over other techniques can be found elsewhere.[8]

The boundary conditions are no-slip conditions for all three velocity components on the surface of either cylinder and periodic conditions for all variables (except pressure) at $Z=0$ and $Z=L$. The solvent viscosity β has been chosen to be 0.59 in order to facilitate comparisons with previous studies.[5] The simulations have been performed for two different meshes with 200 and 400 elements, respectively. Although, changing the mesh size had no significant effect on the results, it was observed that the results (especially in stability analyses) were quite sensitive to the time step size used in the simulations. All the results presented henceforth are for time step size of 0.125 (dimensionless time) and for the smaller mesh. An ensemble size of 2000 trajectories has been used for the configuration fields, although satisfactory results have been obtained with as few as 500 trajectories.

To examine the linear stability of Taylor–Couette flow, the base flow equations [Eqs. (1) and (2)] are linearized. The equation for perturbation stress $\boldsymbol{\tau}_p$ is obtained in the macroscopic case by linearizing the Oldroyd-B constitutive equation

$$\boldsymbol{\tau}_p' + \mathrm{De}\boldsymbol{\tau}_{p(1)}' = \mathrm{De}(-\boldsymbol{u}'\cdot\nabla\boldsymbol{\tau}_p + \boldsymbol{\tau}_p\cdot\boldsymbol{\kappa}'^{\dagger} + \boldsymbol{\kappa}'\cdot\boldsymbol{\tau}_p) + (1-\beta)(\boldsymbol{\kappa}'^{\dagger} + \boldsymbol{\kappa}'). \tag{3}$$

Variables with superscript ($'$) refer to perturbation quantities of the corresponding base flow values.

In the microscopic dumbbells case, one needs to start from the SDE describing the evolution of the connector vectors in order to derive an expression for $\boldsymbol{\tau}_p'$. For example, the linearized equation for the perturbation connector vector $\boldsymbol{Q}'$ for the Hookean dumbbell can be written as

$$d\boldsymbol{Q}' = \left(-\boldsymbol{u}\cdot\nabla\boldsymbol{Q}' - \boldsymbol{u}'\cdot\nabla\boldsymbol{Q} + \boldsymbol{\kappa}'\cdot\boldsymbol{Q} + \boldsymbol{\kappa}\cdot\boldsymbol{Q}' - \frac{1}{2\mathrm{De}}\boldsymbol{Q}'\right)dt.$$

Using the above equation, the evolution equations for $(\boldsymbol{QQ}')$ and $(\boldsymbol{Q}'\boldsymbol{Q})$ can be written for use in determining $\boldsymbol{\tau}_p'$. For example, the SDE for $(\boldsymbol{QQ}')$ is of the form

$$d(\boldsymbol{QQ}') = \Big[-(\boldsymbol{u}\cdot\nabla\boldsymbol{Q})\boldsymbol{Q}' - \boldsymbol{Q}(\boldsymbol{u}\cdot\nabla\boldsymbol{Q}') - \boldsymbol{Q}(\boldsymbol{u}'\cdot\nabla\boldsymbol{Q}) + \boldsymbol{\kappa}\cdot\boldsymbol{QQ}' + \boldsymbol{QQ}'\cdot\boldsymbol{\kappa}^{\dagger} + \boldsymbol{QQ}\cdot\boldsymbol{\kappa}'^{\dagger} - \frac{1}{\mathrm{De}}\boldsymbol{QQ}'\Big]dt + \frac{d\boldsymbol{W}}{\sqrt{\mathrm{De}}}\boldsymbol{Q}'.$$

Now defining the perturbation polymeric stress as $\boldsymbol{\tau}_p' = [(1-\beta)/\mathrm{De}]\langle\boldsymbol{QQ}' + \boldsymbol{Q}'\boldsymbol{Q}\rangle$ and using the definition of the base flow polymeric stress $\boldsymbol{\tau}_p$ from Eq. (11), we get

$$\boldsymbol{\tau}_p' + \mathrm{De}\boldsymbol{\tau}_{p(1)}' = \mathrm{De}(-\boldsymbol{u}'\cdot\nabla\boldsymbol{\tau}_p + \boldsymbol{\tau}_p\cdot\boldsymbol{\kappa}'^{\dagger} + \boldsymbol{\kappa}'\cdot\boldsymbol{\tau}_p) + (1-\beta)(\boldsymbol{\kappa}'^{\dagger} + \boldsymbol{\kappa}'),$$

which is identical to the linearized evolution equation for the perturbation polymeric stresses of an Oldroyd-B fluid [i.e., Eq. (3)]. This demonstrates the viability of our proposed methodology for determining the perturbation polymeric stresses via a stochastic approach.

Similarly, the linearized equation for the perturbation connector vector $\boldsymbol{Q}'$ for the FENE dumbbells can be shown to be

$$d\boldsymbol{Q}' = \left[-\boldsymbol{u}'\cdot\nabla\boldsymbol{Q} - \boldsymbol{u}\cdot\nabla\boldsymbol{Q}' + \boldsymbol{\kappa}'\cdot\boldsymbol{Q} + \boldsymbol{\kappa}\cdot\boldsymbol{Q}' - \frac{1}{2\mathrm{De}}\left(\frac{\boldsymbol{Q}'}{1-\boldsymbol{Q}^2/b} + \frac{2}{b}\frac{(\boldsymbol{Q}\cdot\boldsymbol{Q}')\boldsymbol{Q}}{(1-\boldsymbol{Q}^2/b)^2}\right)\right]dt,$$

and the perturbation polymeric stress, $\boldsymbol{\tau}_p'$ can be obtained by linearizing the corresponding base flow expression for the polymeric stress $\boldsymbol{\tau}_p$.

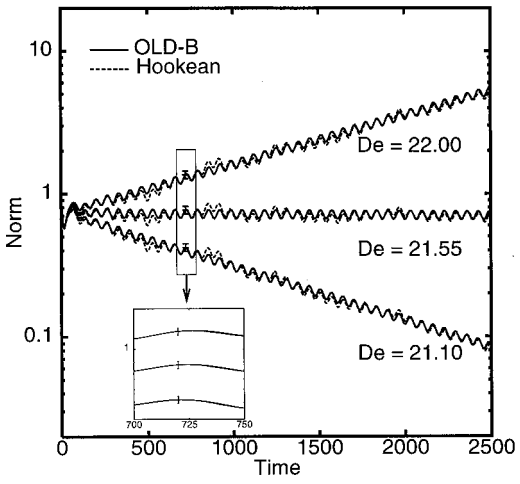

FIG. 1. Evolution of the norm for various values of the Deborah number. The inset shows the statistical error-bar for the Hookean dumbbell simulations.

Axisymmetric two-dimensional small amplitude disturbances in velocity $\boldsymbol{u}'$ are introduced into the governing equations such that, $\boldsymbol{u}'=\phi(r)\exp(i\alpha z)$ where α is the axial wave number and $\phi(r)$ is the amplitude of the disturbance velocity chosen such that $\boldsymbol{u}'$ satisfies continuity requirements and boundary conditions $\boldsymbol{u}'(z,R_1)=\boldsymbol{u}'(z,R_2)=0$. The axial wave number α is set to 7.7 for all the simulations. The choice of wave number is made in order to facilitate quantitative comparisons for the most dangerous eigenvalue obtained from the time-dependent simulations employed in this study and prior GEVP studies.[5]

The evolution of the norm of the solution vector $\boldsymbol{p}$ (defined as $\sqrt{\boldsymbol{p}\cdot\boldsymbol{p}}$) is used to predict the stability characteristics of the flow. If the norm is monitored for sufficiently long times, it settles into an exponentially decaying (or growing) oscillatory behavior. These oscillations are a result of having a nonzero imaginary part of the most dangerous eigenvalue. The long time behavior of the norm is used to evaluate the real part of the most dangerous eigenvalue. The slope of the semilog plot of the norm versus time gives this eigenvalue. Figure 1 shows typical plots of the norms at various values of the Deborah number obtained from both macroscopic (Oldroyd-B) and the corresponding Brownian dynamics (Hookean dumbbell) simulations. As can be seen from the plots, within Brownian fluctuations, there is an exact match between the two. The real part of the most dangerous eigenvalues, obtained as the slopes of these semilog plots, are tabulated in Table I along with those reported in literature using GEVP studies.[5] First, one can observe that the value of the critical Deborah number $\mathrm{De}_c=21.55$ matches well with that previously reported for axisymmetric disturbances.[5] However, a stricter test would be to compare the actual growth rates obtained from the different techniques. It can be seen that, except for De near De_c (i.e., very small growth rates), the match is quite good and the difference can be attributed to the fact that GEVP studies are much more spatially refined. In order to test this hypothesis, we ran one test case (for Oldroyd-B) at De=22.00 and obtained an eigenvalue of $8.14e^{-4}$ which is much closer to the GEVP result than the value reported in Table I. Figures 2(a) and 2(b) show the eigenfunctions corresponding to the perturbation velocity in the r direction, v_r', obtained from both simulations at a dimensionless time $t=1625$. Clearly, the contours are very similar and if followed in time, it is observed that they actually travel in the radial direction which is also in accordance with prior studies.[5] In Table II, the most dangerous eigenvalues obtained from the FENE calculations are presented. We see that the decrease in the finite extensibility predicts greater stability for the system. This is expected, because now there is enhanced shear-thinning and hence the

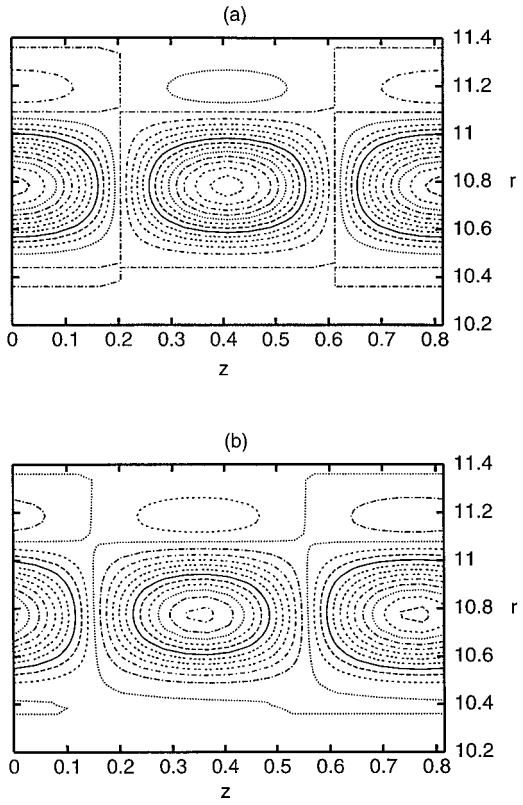

FIG. 2. Eigenfunctions of u_r' for (a) Oldroyd-B fluid and (b) Hookean dumbbells at time=1650.

TABLE I. Most dangerous eigenvalues for different Deborah numbers computed for Hookean (within a statistical error of 4%) and Oldroyd-B cases. OLD-B* values are GEVP results from Ref. 5.

De	Hookean	OLD-B	OLD-B*
21.10	$-9.00e^{-4}$	$-9.00e^{-4}$	$-8.40e^{-4}$
21.55	$-1.20e^{-5}$	$-1.20e^{-5}$	$-8.00e^{-6}$
22.00	$+8.06e^{-4}$	$+8.06e^{-4}$	$+8.20e^{-4}$

TABLE II. Most dangerous eigenvalues (within a statistical error of 4%) for different values of b for FENE dumbbells.

De	$b=5000$	$b=10000$
35.0	$-1.8e^{-1}$	$2.3e^{-3}$
40.0	$-5.8e^{-3}$	$1.2e^{-4}$

Deborah number, having been defined based on the zero-shear rate properties, is effectively decreased providing greater stability.

In conclusion, we have constructed a new technique that allows determination of the hydrodynamic stability of fluids with microstructure using combined finite element/stochastic simulation method. The feasibility of this approach has been demonstrated by examining the linear stability of viscoelastic Taylor–Couette flow using the Hookean and the FENE dumbbell models and comparing the Hookean dumbbell results with its corresponding macroscopic constitutive equation, the Oldroyd-B model. It should be noted that the methodology proposed here is not limited to linear stability analyses and can be easily extended to perform nonlinear stability analyses by time integration of the full nonlinear equations by disturbing the base flow with the most dangerous linearly unstable eigenfunctions. One important issue associated with the present technique is the large CPU time needed to perform the combined Brownian dynamics/finite element simulations. For example, the macroscopic Oldroyd-B stability calculations shown in Fig. 1 take approximately 4 hours to complete, while the corresponding stochastic simulations require ~300 hours on a 533 MHz Alpha system with 1 GB memory. However, it is noteworthy that the most intensive CPU step in the latter simulations is the backsubstitution of the configuration fields, which is trivially parallelizable. We have developed a parallel version of the stochastic simulation code and have observed linear speed-up with number of processors. It is worthwhile to emphasize that, although much more CPU intensive, such techniques are essential in accurately describing the dynamics of the true kinetic theory model. We are presently developing more efficient algorithms to apply this technique to more complex flows.

ACKNOWLEDGMENT

This work has been supported by a grant from the National Science Foundation CTS-97325535.

[1] R. G. Larson, ''Instabilities in viscoelastic flows,'' Rheol. Acta **31**, 213 (1992).
[2] E. S. G. Shaqfeh, ''Purely elastic instabilities in viscometric flows,'' Annu. Rev. Fluid Mech. **28**, 129 (1996).
[3] P. S. Doyle, E. S. G. Shaqfeh, G. H. McKinley, and S. H. Spiegelberg, ''Relaxation of dilute polymeric solutions following extensional flow,'' J. Non-Newtonian Fluid Mech. **76**, 79 (1998).
[4] M. Laso and H. C. Öttinger, ''Calculation of viscoelastic flow using molecular models: The CONNFFESSIT approach,'' J. Non-Newtonian Fluid Mech. **47**, 1 (1993).
[5] U. A. Al-Mubaiyedh, R. Sureshkumar, and B. Khomami, ''Influence of energetics on the stability of viscoelastic Taylor–Couette flow,'' Phys. Fluids **11**, 3217 (1999).
[6] R. B. Bird, C. F. Curtiss, R. C. Armstrong, and O. Hassager, *Dynamics of Polymeric Liquids* (Wiley, New York, 1987), Vol. 2.
[7] M. A. Hulsen, A. P. G. van Heel, and B. H. A. A. van den Brule, ''Simulation of viscoelastic flows using Brownian configuration fields,'' J. Non-Newtonian Fluid Mech. **70**, 79 (1999).
[8] B. Yang and B. Khomami, ''Stability analysis of complex viscoelastic flows using time dependent simulations,'' presented at the 70th Annual Meeting of the Society of Rheology, Monterey, CA, 1998.